The Influence of End Condition on Human Cervical Spine Injury Mechanisms

Roger W. Nightingale

Department of Biomedical Engrg.

Duke University

Brian J. Doherty

Division of Orthopaedic Surgery Baylor University Barry S. Myers and James H. McElhaney

Department of Biomedical Engrg., and Division of Orthopaedic Surgery Duke University Durham, NC

William J. Richardson

Division of Orthopaedic Surgery
Duke University

ABSTRACT

The passive combined flexion and axial loading responses of the unembalmed human cervical spine were measured in a dynamic test environment. The influence of end condition (the degree of constraint imposed on the head by the contact surface) was varied to determine its effect on observed column stiffness and on failure modes of the cervical spine. Multi-axis load cells were used to completely describe the forces and moments developed in the specimen. Twenty three specimens were studied. The Hybrid III neckform performance was assessed to determine its suitability as a mechanical simulator of the neck during head impact. Changes in end condition produced significant changes in axial stiffness in both the Hybrid III neckform and the cadaver neck. The mode of injury also varied as a function of end condition in a repeatable fashion. Separation of injuries based upon imposed end condition identified groups with significantly different axial load to failure. These results also suggest that the risk of cervical injury may be strongly dependent on the degree of head constraint imposed by the contact surface, and that injury environments should be designed to minimize this constraint.

INTRODUCTION

THIS PAPER DESCRIBES the influence of imposed end condition on the structural and failure responses of the unembalmed human cadaver cervical spine in combined compression flexion loading. Implications of these results on compression based injury criteria and the design of safety equipment are also discussed.

Cervical injury remains an important social problem, especially in automotive and aircraft safety. A considerable portion of the literature has been devoted to the characterization of the responses of the cervical spine to loading in the sagittal plane (frontal impacts) and in the coronal plane (side impacts) [1-6]. The kinematics of the cervical spine have been studied in various ways, using static weight pulley, dynamic, and impact test systems [5,7,8]. However, because of the complexity of the spine, much remains unknown regarding its mechanisms of injury and methods for injury prevention.

Studies performed on the human cadaver have identified a large number of variables which influence neck injury. McElhaney et al. [9], noted that in fully constrained tests on isolated cervical spines, small changes in initial position of the head relative to the torso influenced injury mechanism. Nusholtz et al. [5], observed similar results in impacts of whole cadavers. Torg et al. [10], suggested that alignment of the cervical spine to remove the resting lordosis increased the ease with which the cervical spine was injured. Pintar et al. [1], also note the need for preflexion (i.e. removal of the resting lordosis) to create vertebral compression injuries. In contrast, Alem et al. [4], impacting whole cadavers noted that cervical injuries could be produced with the resting lordosis preserved.

The role of head constraint in cervical injury has also been investigated. Roaf [11], was unable to produce lower cervical ligamentous injury in unconstrained flexion. While he suggested that axial torsion was the mechanism of lower cervical ligamentous injury, subsequent work by Myers et al. [12], has mitigated the role of torsion in lower cervical injuries. Hodgson and Thomas [13] suggested that restriction of motion of the atlantoaxial joint greatly increased the risk of injury. Bauze and Ardran [14], produced bilateral facet dislocation in the cadaver by constraining rotation of the head, and inserting a peg in the neural foramen. Yoganandan et al. [15], noted that head constraint increased the measured axial load and the number of injuries in cadaver impacts. Doherty et al. [8], and McElhaney et al. [2], have shown that changes in the imposed end condition increased the observed axial and flexural stiffness of the cervical spine; and that these changes were significantly greater than those predicted by elementary beam theory. Liu and Dai [16], based on a theoretical analysis of a beam-column, suggest that the second stiffest axis may play a role in injury. Very few performance standards (restraint system or helmet) consider cervical spine protection and tolerance. The only ones we are aware of are Mertz and Patrick [17], and the industrial helmet standard ANSI Z89.

Mechanical analysis based upon the effective mass of the torso, and the energy absorption of the neck reveals that the cervical spine is capable of managing impacts equivalent to vertical drop of 0.50 meters when the neck is called upon to stop the torso [18]. Unfortunately, many impact situations have considerably larger impact energies. In these situations, the head-neck complex must either move out of the path of, or be at risk for injury from, the momentum of the impinging torso. Based on these considerations, the purpose of this paper is to examine the effect of imposed end condition, the degree of head constraint, on the observed axial stiffness of the cervical spine, and on the risk of cervical injury.

METHODS

SPECIMEN TYPES AND PROCUREMENT - Unembalmed human cervical spines were obtained shortly after death, sprayed with calcium buffered isotonic saline, sealed in plastic bags, frozen and stored at -20 degrees Celsius. Cervical spine specimens included the base of the skull through to the first thoracic vertebra (T1). All ligamentous structures were kept intact, with the exception of the ligamentum nuchae. Medical records of donors were examined to ensure that the specimens did not show evidence of serious degenerative disease, spinal disease, or other health related problems that would affect their structural responses. A total of 18 specimens were used in these experiments. Specimen ages varied from 40 to 75 years. Pretest A-P and lateral radiographs were performed prior to casting to rule out the possibility of pre-existing spinal pathology.

SPECIMEN PREPARATION -Prior to testing, each specimen was thawed at 20 degrees Celsius for 12 hours in a 100 percent relative humidity environment. The end vertebra were cleaned, dried and defatted for casting. Specimens were cast into aluminum cups with reinforced polyester resin so that the cup ends were parallel under no load. The cup centers were aligned along the center of the neural canal. Casting of the thoracic end of the specimen was performed such that the T1 vertebra was oriented at approximately 25 degrees to the horizontal plane, this preserved the resting lordosis of the spine. Screws were inserted into the T1 vertebral body and posterior elements of T1 so that the T1 vertebra only partially inserted into the resin of the lower cup. This ensured that the C7-T1 motion segment was clear of the cup surface. During casting, the aluminum cups were cooled in a flowing water bath to dissipate the heat of polymerization.

TEST INSTRUMENTATION - Tests were conducted with an MTS servo-controlled hydraulic testing machine composed of a load frame with linear actuator, a 25 gpm, 3000 psi hydraulic pump, two nitrogen filled accumulators and a linear feedback control system. Loads were measured at the caudal end of the specimen using a six axis array of strain gauge load cells composed of two GSE three-axes ATD neck load cells and a GSE torsion cell, arranged to quantify force and moment in three orthogonal axes. The caudal end of the specimen was fixed to the upper platen of the MTS. A system of linkages imposed a variety of different end conditions on the base of skull. Sagittal plane motion at the base of the skull was described using linear variable differential transformers (LVDT) and a rotational variable differential transformer (RVDT) as was required to fully describe the motion of the head relative to the fixed thoracic end for each end condition investigated. An MTS digital function generator and controller were used to apply waveforms to the linear actuator. In addition, in situ fluoroscopic images of the cadaver tests, and videotape images of the Hybrid III neckform [19] tests were recorded during testing.

A digital measurement and analysis system was developed utilizing a data logging computer to record the nine channels of transducer output. The multichannel microcomputer data acquisition system incorporated an RC-Electronics ISC-67 Computerscope for the digitization and storage of data. This system, which consists of a 16-channel A/D board, an external instrument interface box, and Scope Driver software, has a 1 MHz aggregate sampling rate, 12 bit resolution and writes data directly to a hard disk. Data analysis was performed on a Sun workstation.

EXPERIMENTAL METHODS – The thoracic cup was rigidly connected to the upper platen of the MTS. Three different end conditions were imposed on the head (base of skull) cup to represent the spectrum of head end conditions seen in the accident environment. The three end conditions investigated, and the motions they impose, are shown in Figure 1 and are denoted: unconstrained, rotation constraint, and full constraint. The reference axes used for these tests are spatially fixed to the centroid of the load cell, and are shown in Figure 2. The term 'axial' is used in this text to refer to loads and deflections in the 'z' (vertical) direction.

The first set of tests consisted of non-destructive testing of five specimens to determine the influence of end condition on axial stiffness. A preload equal to the weight of the head and neck was applied to each specimen and the amplifiers balanced so that the load cell showed no axial load, P, at the beginning of each test. A cyclic axial displacement using a 1 Hz haversine and the unconstrained end condition was applied for 50 cycles to exercise the specimen and place it in a mechanically stabilized (reproducible) state [9]. This was necessary so as to reduce the transient stiffening effects associated with prolonged (greater than 12 hours) inactivity [9]. A constant velocity axial displacement was then applied to the head over a 2.0 second interval for each end condition. The magnitude of the axial displacement was estimated to produce approximately 200 N of axial load. For comparison purposes axial stiffness was determined using a secant method defined by the axial deflection which occurred over an axial load range of from 0 to 200 N. Estimation of the C6-C7 motion segment flexion moment was accomplished using the initial position of the C6-C7 vertebral disk relative to the load cell and the following equation, derived from the free body diagram shown in Figure 2:

$$M_{6-7} = M_t + VB - PA \tag{1}$$

The second group of tests consisted of load to failure testing of 18 specimens. The specimens were divided amongst the unconstrained, rotational constraint and full constraint end condition. Data collected from McElhaney et al. [9], served to augment the full constraint end condition results. Each specimen was mechanically stabilized using the cyclic test described above, and the unconstrained end condition. To fail the specimen, a constant velocity axial displacement was performed using a 2.0 second ramp. The magnitude of the applied displacement was 9.0 cm for the unconstrained end condition, 4.0 cm for the rotational constraint end condition, and 2.0 cm for the full constraint end condition. The magnitude of the applied displacement was scaled based on the ratio specimen length against a mean specimen length of 18 cm, to give equal applied displacements as a percentage

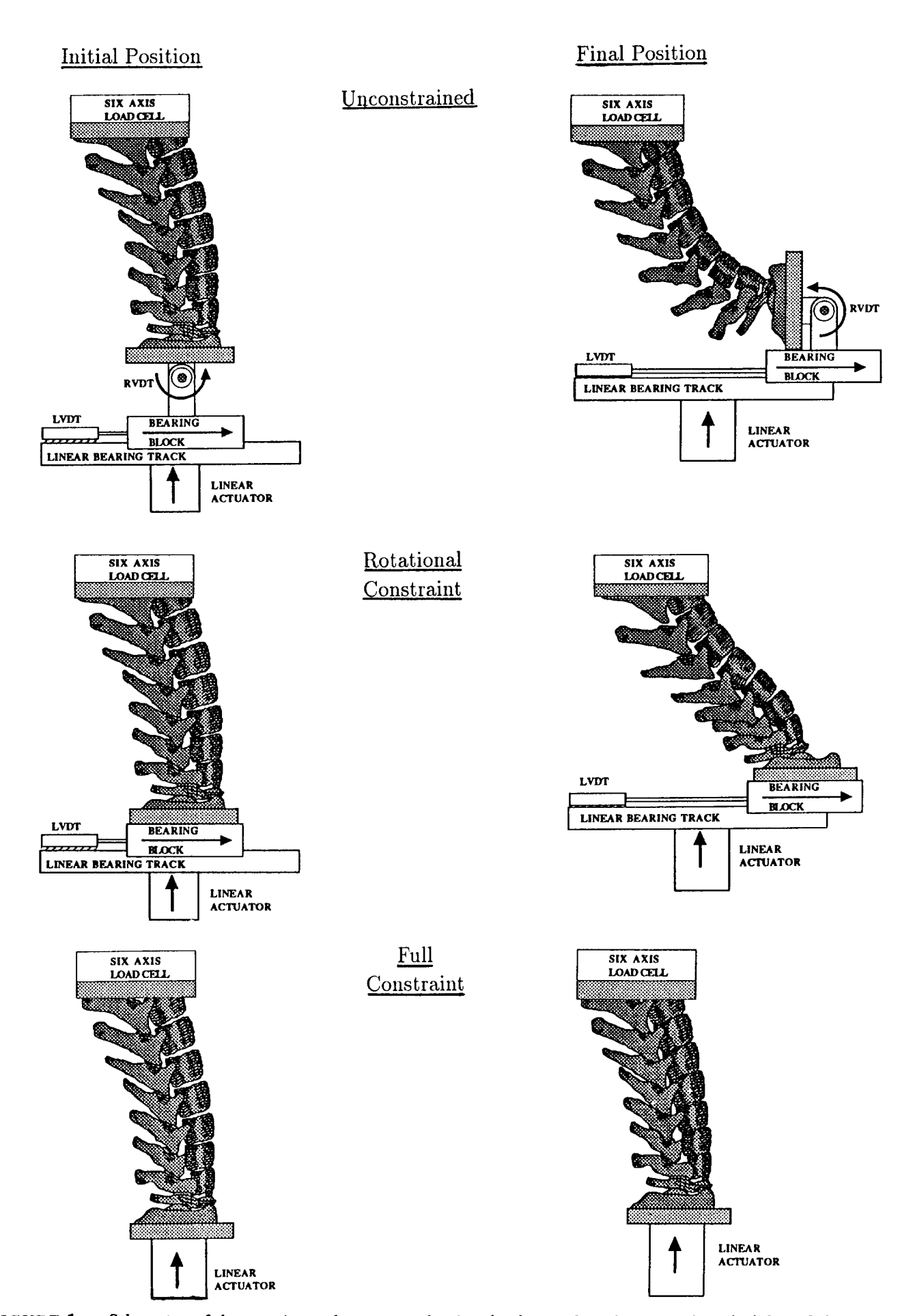


FIGURE 1. Schematics of the experimental apparatus showing the three end conditions used on the left, and the motions which result from the applied axial displacements on the right.

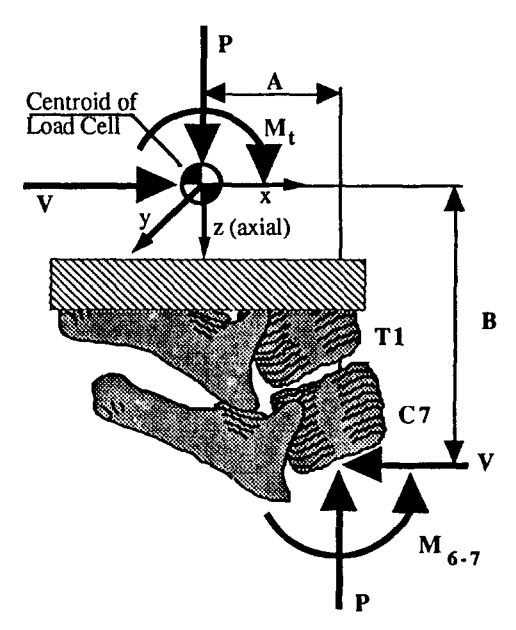


FIGURE 2. Free body diagram showing the method used for estimation of the C6-C7 bending moment from the load cell data, and the reference axes. P denotes axial compression force, V denotes a shearing force, and M denotes a flexion bending moment. A and B are the distances from the centroid of the load cell to the center of the C6-C7 intervertebral disk.

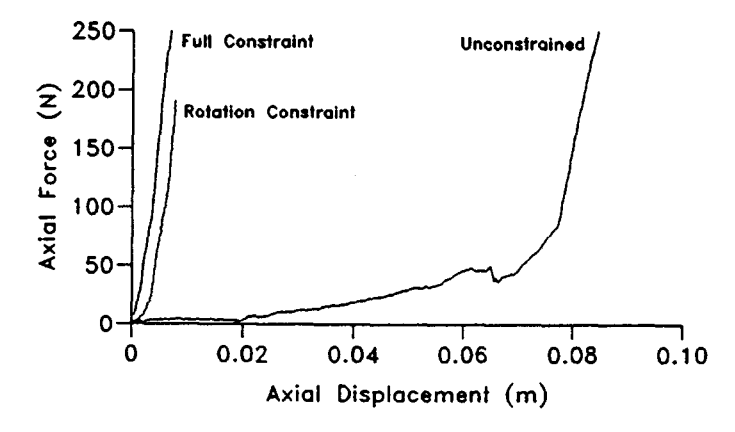


FIGURE 3. Influence of end condition on the axial load-deflection history for a typical specimen.

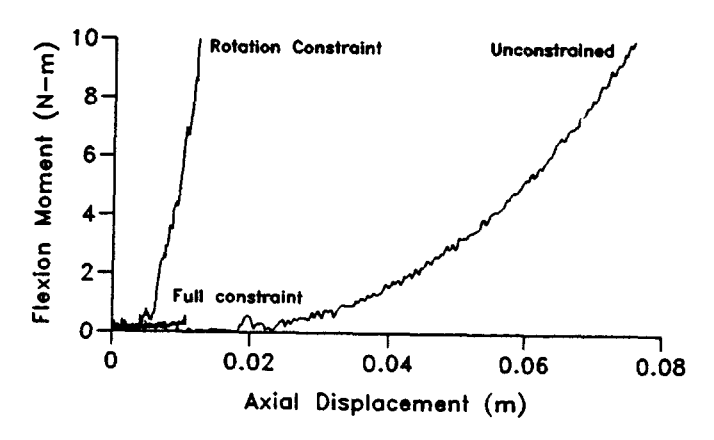


FIGURE 4. Influence of end condition on the flexion moment-axial deflection history for a typical specimen.

of specimen length for each specimen. Following loading, the specimen was removed from the actuator and failures were documented by magnetic resonance, computerized tomography, and physical dissection.

The test battery, including mechanical stabilization, and evaluation with each end condition was also performed on the Hybrid III neckform. The calculation of the flexion moment was performed at the base of the Hybrid III neckform.

TEST RESULTS

STIFFNESS TESTS - Qualitative analysis of fluoroscopic images revealed the expected kinematics of the spine associated with each end condition. Eccentricity, the effective bending moment arm for the resultant axial load, was defined as the horizontal distance from the center of the foramen magnum to the center of the C6-C7 vertebral disk. In the unconstrained group and the rotational constraint group, the applied axial displacement resulted in anterior translation of the head relative to the fixed thorax. The result was an increase in the eccentricity of the axial load. In the unconstrained group, the head was also free to rotate with applied axial deflection. In the full constraint group, no motion other than superior inferior translation was permitted. All specimens remained in the sagittal plane during axial loading, in the absence of significant constraint of out of plane motions.

Changes in axial stiffness were observed with the different end conditions. Increasing the degree of imposed constraint increased the observed axial stiffness in all five specimens. Figure 3 shows the influence of end condition on the axial load-deflection history for a typical specimen. Mean axial stiffness increased by a factor of 8.5 between unconstrained and rotational constraint end conditions, and by a factor of 12.2 between unconstrained and full constraint end conditions (Table 1).

The C6-C7 flexion moment resulting from the applied axial displacement was also affected by end condition. Unconstrained specimens had a significant "no moment" region with subsequent development of flexion moments at large displacements. Rotational constraint specimens developed large flexion moments at small axial displacements due to a moderate axial stiffness, large eccentricity, and no anterior to posterior shearing force. Full constraint specimens had small flexion moments despite a large axial stiffness, due to the development of an anterior to posterior shearing force which opposed flexion, and the small eccentricity of the resultant axial load (Figure 4). Figure 5 shows the change in eccentricity with applied axial displacement for each end condition for a typical cervical spine.

To summarize, full constraint produced large axial loads and comparatively small flexion moments when subjected to axial displacement. Rotational constraint produced moderate axial loads, and comparatively large flexion moments and the unconstrained specimens developed small axial loads and small flexion moments.

TABLE 1

THE EFFECT OF END CONDITION ON AXIAL STIFFNESS AT LOW LOADS

SPECIMEN #	UNCONSTRAINED (kN/m)	ROTATIONAL CONSTRAINT (kN/m)	FULL CONSTRAINT (kN/m)
1	4.46	54.6	95.5
2	3.93	22.4	24.3
3	2.21	27.2	26.1
4	4.21	25.6	41.0
5	1.97	12.2	18.2
Cadaver Average	3.36 ± 1.17	28.4 ± 15.8	41.0 ± 31.9
HYBRID III	169.2	336.4	416.5
HYBRID III to cadaver ratio	50.3	11.8	10.2

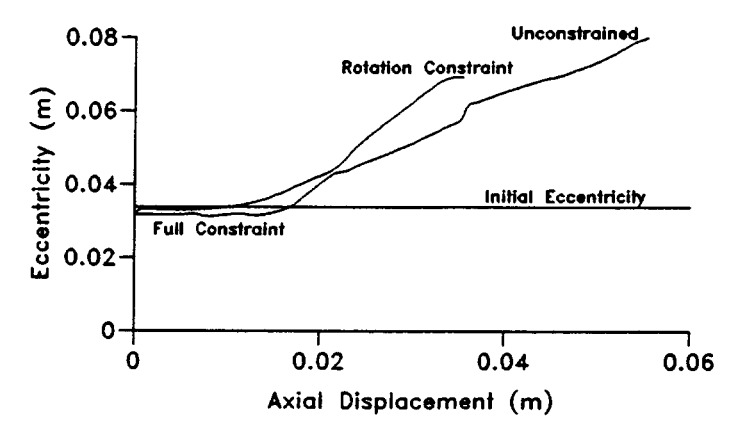


FIGURE 5. Change in eccentricity, the bending moment arm for the axial load, as a function of end condition for a typical cadaveric specimen. Note that in the full constraint end condition the eccentricity is constant.

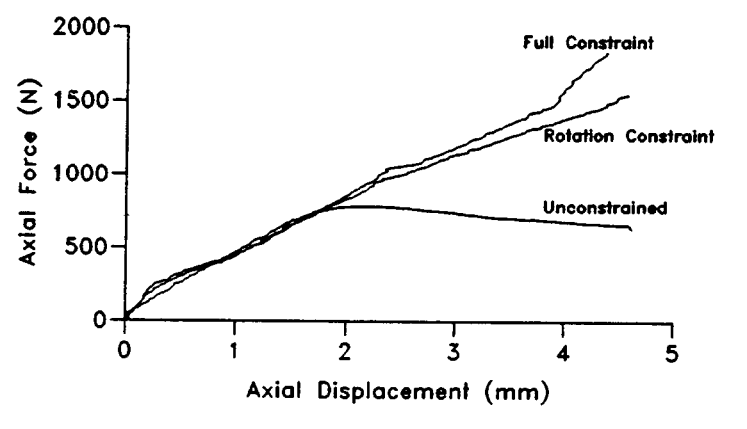


FIGURE 6. Influence of end condition on the axial load-deflection history for the Hybrid III neckform.

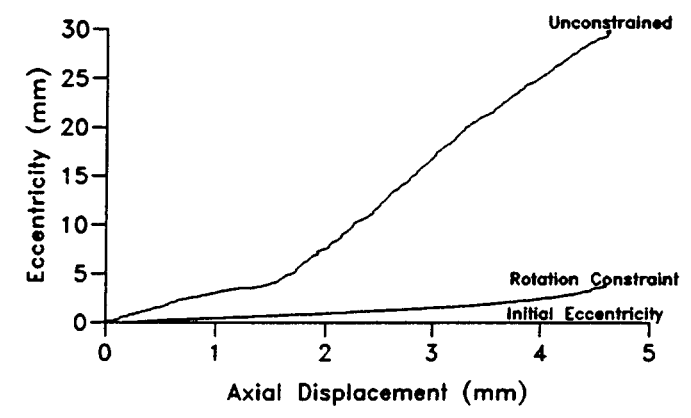


FIGURE 7. Change in eccentricity as a function of end condition for the Hybrid III neckform. The figure shows the absence of an initial eccentricity in all end conditions, and no eccentricity developing in the full constraint end condition.

The Hybrid III neckform was 10.2 to 50.3 fold stiffer than the human cadaver cervical spine depending on the imposed end condition (Table 1). The influence of end condition on the axial load—deflection history of the Hybrid III neckform is shown in Figure 6, on the eccentricity in Figure 7, and on the flexion moment in Figure 8. The unconstrained end condition developed larger flexion moments than the rotational constraint end condition, unlike the cadaver. This was due to the relatively small change in eccentricity with rotational constraint in the Hybrid III neckform as compared to the human cadaver (Figures 5 and 7).

FAILURE TESTS – End condition influenced the risk of injury, the failure mode, and the observed axial load to failure. In the full constraint group both upper and lower cervical injuries were observed. In this study only the lower cervical injuries have been included. Full constraint showed the largest axial stiffness, and the largest axial loads at failure. A mean peak axial load of 4810 ± 1290 N was measured at a mean axial displacement of 1.4 ± 0.4 cm. Compression and wedge compression injuries were produced. No dislocations or significant ligamentous injuries were observed in any of the specimens in this group.

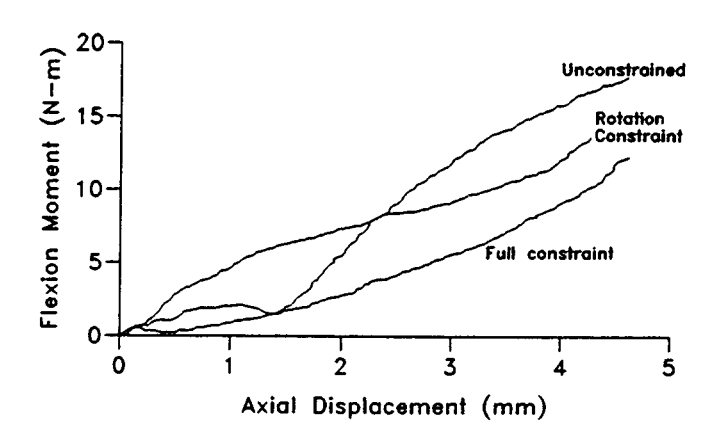
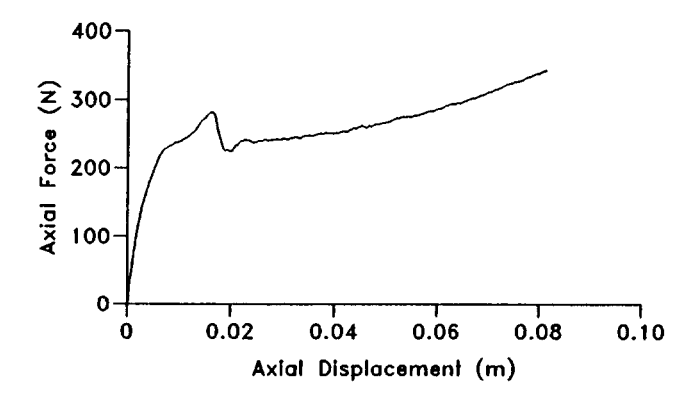


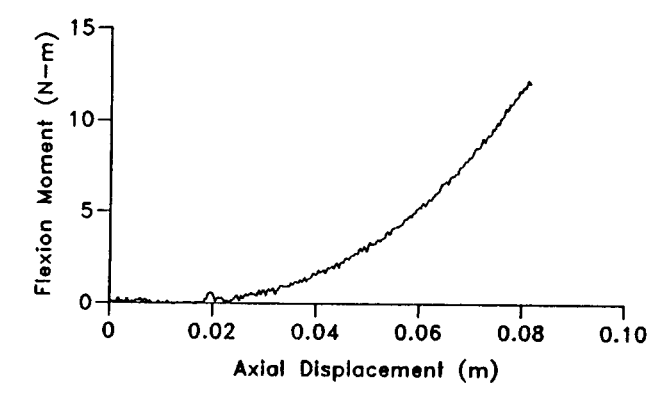
FIGURE 8. Change in flexion moment for the Hybrid III neckform as a function of end condition. Note the abrupt increase in flexion moment in the unconstrained end condition at approximately 1.5 mm of axial displacement indicative of buckling.

In the rotational constraint group, bilateral facet dislocation of the lower cervical spine was observed with posterior ligamentous and intervertebral disk disruption in each of the six specimens. No evidence of vertebral body compression injury was observed by dissection or imaging. Clear evidence of catastrophic failure was observed on the axial load–deflection data. Mean peak axial load to bilateral facet dislocation was 1720 \pm 1230 N at a mean axial displacement of 2.9 \pm 0.9 cm. Bending moments at failure were large due to the eccentric axial load and the absence of an anterior to posterior shearing force.

In the unconstrained group, the applied axial displacement was sufficiently large to place the chin (if it were present) through the sternum, and anterior portions of the thoracic vertebral bodies. These unconstrained specimens showed a large initial low stiffness region, and correspondingly small axial loads. Mean peak axial load was 289 ± 81.4 N at a mean axial displacement of 8.6 ± 1.8 cm and a total of 96 ± 7.3 degrees of rotation of the head relative to T1. Despite this applied axial displacement, no evidence of significant structural injury was observed by plain X rays, CT, MRI or physical dissection in all six specimens studied.

Evidence suggestive of failure (decreasing axial force with increasing deflection) was occasionally seen on the axial force-deflection history at low loads in the unconstrained end condition. Analysis of axial force-deflection, eccentricity-deflection, and moment-deflection data showed evidence of buckling of the cervical spine from a compression mode to a flexion mode when this decrease occurred (Figure 9). The Hybrid III neckform also buckled from a compression mode to a flexion mode with the unconstrained end condition, though at a considerably higher load (780 N). This is seen in Figures 6, 7 and 8 at an axial displacement of 1 to 2 mm, and was observed on the videotape. Figure 6 shows the decrease in load with increasing deflection. Figure 7 shows an abrupt change in the rate of development of eccentricity with axial displacement and Figure 8 shows an increase in the rate of flexion moment development with axial displacement.





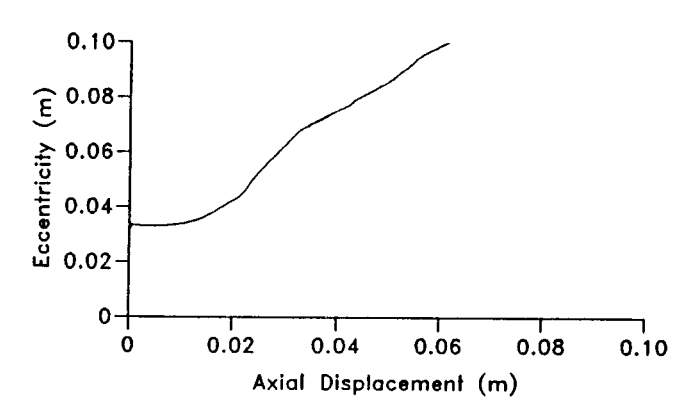


FIGURE 9. Three figures from a cadaveric specimen failure test with an unconstrained end condition showing evidence of low load buckling from a compression mode to a flexion mode. The figures show an abrupt decrease in the rate of development of axial load, and an increase in the rate of development of flexion moment and eccentricity occurring at approximately 0.016 m of axial displacement, indicative of buckling.

The device was undamaged by the loading, and subsequently carried larger loads at larger displacements. In addition, the event was reproducible, suggesting that it represented a buckle with post-buckling stability in the flexion mode.

Table 2 summarizes the injuries produced, and lists the measured peak axial loads, the axial displacements and strain energies to failure for all specimens studied. Figure 10 compares the load–deflection characteristics for three typical specimens. Using a student t-test, the rotational constraint group was found to have a significantly lower axial load to failure than the full constraint group (p < 0.01). The peak loads of the unconstrained group were also significantly lower than the rotational constraint group (p < 0.01).

TABLE 2

THE EFFECT OF END CONDITION ON FAILURE LOAD AND MECHANISM

END CONDITION unconstrained	PEAK AXIAL LOAD (N)	AXIAL DEFLECTION	ENERGY AT	
			FAILURE	INJURY
unconstrained	(11)	(cm)	(N-m)	INJUNI
unconsumited	365	5.8	#4.2	None
unconstrained	367	10.2	#5.0	None
unconstrained	240	10.8	#6.1	None
unconstrained	343	8.2	#21.0	None
unconstrained	169	8.6	#9.9	None
unconstrained	250	8.2	#17.8	None
unconstrained	289 ± 81.4	8.6 ± 1.8	#11.5 ± 6.5	
otation constraint	3590	3.6	14.6	*BFD C5-C6
otation constraint	2950	3.3	46.9	*BFD C6-C7
otation constraint	1130	2.9	20.7	*BFD C7-T1
otation constraint	1110	2.3	11.7	*BFD C7-T1
otation constraint	600	1.5	4.8	*BFD C7-T1
otation constraint	930	3.9	11.9	*BFD C7-T1
otation constraint	1720 ± 1234	2.9± 0.9	26.8 ± 23.7	
full constraint	5340	2.5	85.5	C2 comp. fx.
full constraint	4060	1.2	21.3	C3 comp. fx.
full constraint	6840	1.2	42.0	C4 & C5 wedge comp. fx.
full constraint	4700	1.2	32.9	C4 & C5 comp. fx.
full constraint	3000	1.7	26.1	C3 & C6 comp. fx.
full constraint	4940	1.1	21.5	C4 wedge comp. fx.
full constraint	4810 ± 1286	1.4 ± 0.4	32.9 ± 12.8	
	unconstrained unconstrained unconstrained unconstrained unconstrained unconstrained unconstrained unconstrained unconstrained tation constraint tation constraint tation constraint tation constraint tation constraint tation constraint full constraint full constraint full constraint full constraint full constraint	unconstrained 367 unconstrained 240 unconstrained 343 unconstrained 169 unconstrained 250 unconstrained 289 ± 81.4 particular constraint 3590 particular constraint 2950 particular constraint 1130 particular constraint 600 particular constraint 930 particular constraint 1720 ± 1234 full constraint 4060 full constraint 6840 full constraint 4700 full constraint 4940 full constraint 4940 full constraint 4810 ± 1286	unconstrained 367 10.2 unconstrained 240 10.8 unconstrained 343 8.2 unconstrained 169 8.6 unconstrained 250 8.2 unconstrained 289 ± 81.4 8.6 ± 1.8 station constraint 3590 3.6 station constraint 2950 3.3 station constraint 1130 2.9 station constraint 1110 2.3 station constraint 600 1.5 station constraint 930 3.9 station constraint 1720 ± 1234 2.9± 0.9 full constraint 5340 2.5 full constraint 4060 1.2 full constraint 4700 1.2 full constraint 4700 1.2 full constraint 4940 1.1 full constraint 4810 ± 1286 1.4 ± 0.4	unconstrained 367 10.2 #5.0 unconstrained 240 10.8 #6.1 unconstrained 343 8.2 #21.0 unconstrained 169 8.6 #9.9 unconstrained 250 8.2 #17.8 unconstrained 289 ± 81.4 8.6 ± 1.8 #11.5 ± 6.5 tation constraint 3590 3.6 14.6 tation constraint 2950 3.3 46.9 tation constraint 1130 2.9 20.7 tation constraint 1110 2.3 11.7 tation constraint 600 1.5 4.8 tation constraint 930 3.9 11.9 tation constraint 1720 ± 1234 2.9 ± 0.9 26.8 ± 23.7 full constraint 5340 2.5 85.5 full constraint 4060 1.2 21.3 full constraint 4700 1.2 32.9 full constraint 4940 1.1 21.5 <

^{*}BFD = bilateral facet dislocation.

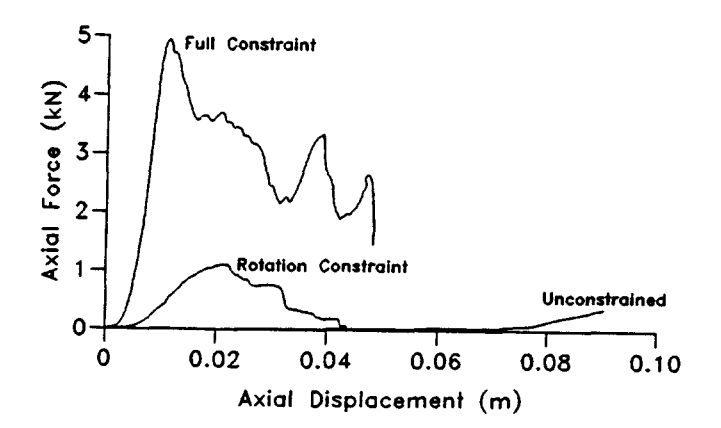


FIGURE 10. Comparison of typical axial load-deflection histories for three different cadaveric specimens loaded to failure with three different end conditions.

DISCUSSION

It is apparent from previous investigations that the neck is unable to stop the moving torso for all but the slowest velocities. Accordingly, in the injury environment, the head-neck complex must either move out of the way of the impinging torso or be at risk for injury.

Numerous investigations have been performed to understand the mechanisms of injury of the cervical spine. Based on these experiments a number of variables have been identified which predispose the spine to injury [5,9]. These include the initial position of the neck, the presence of a preflexed spine and the degree of the imposed head constraint. The purpose of these experiments was to create a set of end conditions which reasonably recreated the spectrum of end conditions imposed in the injury environment. The end conditions studied account for the degree of constraint imposed by the contact surface, and the trajectory of the thorax relative to the head.

Imposition of different end conditions resulted in large changes in the observed axial stiffness of the cervical spine within a given specimen. This was consistent with our previous work [2,8,9]. End condition also influenced the risk for injury. In the absence of significant constraint, the stiffness of the structure was low,

[#]Values denote stored strain energy.

the spine was able to flex out of the way of the torso and no injuries were observed. Increasing the constraint resulted in increased axial stiffness of the structure, but, the stiffened structure was neither able to manage the equivalent energy of a moving torso nor get out of the way of the torso.

This data suggests that increasing the constraint on the head increases the likelihood of neck injury. It also suggests that employment of deformable contact surfaces which do not manage the impact energy to reduce the force of impact, but, impose a significant head constraint, may be placing the neck at risk for injury. These results should be tempered however, realizing that the experiments discussed here were conducted at a low rate relative to real accidents. While the lower rate allowed for greater control of the end conditions, it neglects the potential contributions of inertial loading to the injury modes. Future work at higher rates of loading is therefore recommended to validate this hypothesis.

Each imposed end condition resulted in a repeatable injury mechanism. That is, rotational constraint, which might occur during impact of the head into a compliant surface with the torso moving posteriorly, resulted in bilateral facet dislocation in 6 of 6 specimens studied. Full constraint, which might occur when the head pockets in the contact surface and the trajectory of the torso is collinear with the axis of the neck, resulted in a compression type of injury in 6 of 6 specimens. Unconstrained, or a free end condition, resulted in no injury in 6 of 6 specimens. Of note, it was not necessary to preflex the spine to produce these injuries.

Buckling was observed in the unconstrained end condition in both the human cadaver, and the Hybrid III neckform at comparatively low axial loads. Analysis of the data, and the in situ video images showed that this represented first mode buckling from compression to flexion. The absence of injury in the specimens and the repeatabliity of the event in the Hybrid III neckform demonstrate that this event represents buckling with postbuckling stability. In the cadaver the axial load required to produce this event was of the same order as the weight of the head, suggesting that the in vivo cervical spine may be in a stable post-buckled condition. More importantly, the event was a first mode buckle with a free end condition; beam theory would suggest therefore that higher load, higher mode, potentially injurious buckling conditions may exist. The contributions of these modes, if they exist, to injury mechanics represents a topic of further investigation.

Understanding the basis for the structural failure of the neck remains a problem for biomechanical engineering. Much has been learned about injury by experiments performed in the cadaver. These tests are however, difficult to perform, show a large interspecimen variation, and are limited in the number which can be performed on a given specimen. The presence of nonlinear viscous effects, and buckling modes serve only to increase the complexity of the analysis. While the Hybrid III neckform was able to recreate some of these effects, most notably, the buckling of the unconstrained specimen, its was stiffer than the cadaver in the axial direction in all three end conditions. For the unconstrained, and rotational constraint end conditions, these differences are to be expected however, as the reported axial stiffnesses include contributions of both compression and flexion. The Hybrid III neckform correctly includes the stiffening effects of the active musculature in flexion, while the cadaver lacks these effects. In the full constraint end condition, which represents a nearly pure compression mode of loading, the contributions of the musculature are comparatively small, and the cadaver response approaches the volunteer response [20]. This suggests that the Hybrid III neckform is stiffer along its axis than the cervical spine. This result is consistent with the values reported by Yoganandan et al.[3]. Given the importance of compressive loading to cervical injury, particularly in non-automotive sources of cervical injury (i.e. sporting events and dives), the availability of a high biofidelity head–neck for compression would be of great benefit to the design and evaluation of safety equipment.

CONCLUSIONS

- 1. The imposed end condition reliably alters the failure mechanism of the cervical spine. This preliminary data suggests that safety equipment, and injury environments should be designed to minimize the degree of imposed constraint on the head. In particular, systems which tend to "pocket" without providing adequate energy management may provide an enhanced injury potential. As discussed, further work is necessary to better validate this conclusion.
- 2. The axial load to failure for lower cervical bilateral dislocation is significantly lower than the axial load to failure for vertebral compression type fractures.
- 3. First mode buckling can occur at very low loads in unconstrained specimens. The resulting structure is however, stable, and uninjured. The existence of other buckling modes and their contribution to cervical injury mechanics is unknown. Interpretation of failure data as defined by decreases in the axial load with increasing axial deflection are therefore difficult, given the frequent absence of significant mechanical injury, and the presence of buckling effects.

ACKNOWLEDGMENT

This study was supported by the Department of Health and Human Services, Centers for Disease Control Grant R49/CCR402396-02, and the Virginia Flowers Baker Chair.

BIBLIOGRAPHY

- Pintar, F., Sances, A. Jr., Yoganandan, N., Reinartz, J., Maiman, D.J., Suh, J.K., Unger, G., Cusick, J.F., and Larson, S.J., "Biodynamics of the Total Human Cervical Spine," The 32nd Stapp Car Crash Conference, 55-72, 1990.
- McElhaney, J.H., Doherty, B.J., Paver, J.G., Myers, B.S., and Gray, L., "Combined Bending and Axial Loading Responses of the Human Cervical Spine," The 32nd Stapp Car Crash Conference, 21-28, 1988.
- 3. Yoganandan, Sances, A. Jr., N., and Pintar, F., "Biomechanical Evaluation of the Axial Compressive Responses of the Human Cadaveric and Manikin Necks," *Journal of Biomechanical Engineering*, 111:250–255, 1989.

- 4. Alem, N.M., Nusholtz, G.S., and Melvin, J.W., "Head and Neck Response to Axial Impacts," *The 28th Stapp Car Crash Conference*, 275-287, 1984.
- Nusholtz, Huelke, D.E., Lux, P., Alem, N.M., and Montalvo, F., "Cervical Spine Injury Mechanisms," The 27th Stapp Car Crash Conference, 179-197, 1983.
- Morgan, R.M., Marcus, J.H., and Eppinger, R.H., "Side Impact - The Biofidelity of NHTSA's Proposed ATD and Efficacy of TT1," The 25th Stapp Car Crash Conference, 301, 1981.
- 7. White A.A., and Panjabi, M.M., Biomechanics of the Spine, Lippincott Publishers, Philadelphia, 1978.
- 8. Doherty, B.J., McElhaney, J.H., and Myers, B.S., 'The Effect of End Conditions on the Responses of the Cervical Spine to Complex Loading," *Journal of Biomechanics*, submitted for review, 1991.
- 9. McElhaney, J.H., Paver, J.G., McCrackin, H.J., and Maxwell, G.M., "Cervical Spine Compression Responses", The 27th Stapp Car Crash Conference. 163-177, 1983.
- 10. Torg, J.S., Athletic Injuries to the Head, Neck and Face. Lea and Febiger, Philadelphia, 1982.
- 11. Roaf, R., "A Study of the Mechanics of Spinal Injury," Journal of Bone and Joint Surgery, 42B:810-823, 1960.
- 12. Myers, B.S., McElhaney, J.H., Doherty, B.J., Paver, J.G., and Gray, L., "The Role of Torsion in Cervical Spinal Injury" *Spine*, 16(8):870-874, 1991.

- 13. Hodgson, V.R., and Thomas, L.M., "Mechanisms of Cervical Spine Injury During Impact to the Protected Head," Society of Automotive Engineers Transactions, Paper #801300, 17-42, 1980.
- Bauze, R.J., and Ardran, G.M. "Experimental Production of Forward Dislocation of the Human Cervical Spine." The Journal of Bone and Joint Surgery, 60B:239-245, 1978.
- 15. Yoganandan, N., Sances, A. Jr., Maiman, D.J., Myklebust, J.B., Pech. P., and Larson, S.J., "Experimental Spinal Injuries with Vertical Impact," *Spine*, 11(9):855-860, 1986.
- 16. Liu, Y.K., and Dai, Q.G., "The Second Stiffest Axis of A Beam Column: Implications for Cervical Spine Trauma." *Journal of Biomechanical Engineering*, 111:122-127, 1989.
- Mertz, H.J., and Patrick, L.M., "Strength and Response of the Human Neck," The 15th Stapp Car Crash Conference, SAE Paper No.710855, 1971.
- 18. McElhaney, J.H., Snyder. R.G., States, J.D., and Gabrielsen, M.A. "Biomechanical Analysis of Swimming Pool Injuries." *Society of Automotive Engineers*, paper no. 790137, 47-53, 1979.
- Foster, J.K., Kortge, J.O., and Wolanin, M.J., "Hybrid III A Biomechanically-Based Crash Test Dummy," The 21st Stapp Car Crash Conference, 975-1014, 1977.
- Wismans, J., Philippens. M., van Oorschot. E., Kallieris, D., and Mattern. R. "Comparison of Human Volunteer and Cadaver Head-Neck Response in Frontal Flexion." The 31st Stapp Car Crash Conference, 1-11, 1987.